Erica Pack
School of Plant and Environmental Sciences,
Virginia Tech,
Blacksburg, VA 24061;
STRETCH Lab,
Department of Biomedical Engineering and
Mechanics, and School of Plant and
Environmental Sciences,
Virginia Tech,
Blacksburg, VA 24061
e-mail: edpack@vt.edu

Justin Dubik
STRETCH Lab,
Department of Biomedical
Engineering and Mechanics,
Virginia Tech,
Blacksburg, VA 24061
e-mail: jrdubik@vt.edu

William Snyder
STRETCH Lab,
Department of Biomedical
Engineering and Mechanics,
Virginia Tech,
Blacksburg, VA 24061
e-mail: swilli9@vt.edu

Alexander Simon
Department of Biomedical
Engineering and Mechanics,
Virginia Tech,
Blacksburg, VA 24061
e-mail: alex34@vt.edu

Sherrie Clark
Department of Large Animal Clinical Sciences,
Virginia-Maryland College of
Veterinary Medicine,
Virginia Tech,
Blacksburg, VA 24061
e-mail: sherrie@vt.edu

Raffaella De Vita
STRETCH Lab,
Department of Biomedical
Engineering and Mechanics,
Virginia Tech,
Blacksburg, VA 24061
e-mail: devita@vt.edu

Biaxial Stress Relaxation of Vaginal Tissue in Pubertal Gilts

Pelvic organ prolapse (POP) is a condition characterized by displacement of the vagina from its normal anatomical position leading to symptoms such as incontinence, physical discomfort, and poor self-image. Conservative treatment has shown limited success and surgical procedures, including the use of mesh, often lead to severe complications. To improve the current treatment methods for prolapse, the viscoelastic properties of vaginal tissue need to be characterized. We determined the biaxial stress relaxation response of vaginal tissue isolated from healthy pubertal gilts. Square specimens (n = 20) with sides aligned along the longitudinal directions (LD) and circumferential direction (CD) of the vagina were biaxially displaced up to 5 N. The specimens were then kept at the displacements corresponding to 5 N for 20 min in both the LD and CD, and the corresponding strains were measured using digital image correlation (DIC). The stresses in the LD and CD were found to decrease by 49.91 ± 5.81% and 46.22 ± 5.54% after 20 min, respectively. The strain in the LD and CD increased slightly from 0.080 ± 0.054 to 0.091 ± 0.064 and 0.050 ± 0.039 to 0.058 ± 0.047, respectively, but these changes were not significant (p > 0.01). By using the Peleg model, the initial decay rate and the asymptotic stress during stress relaxation were found to be significantly higher in the LD than in the CD (p ≪ 0.001), suggesting higher stress relaxation in the LD. These findings may have implications for improving current surgical mesh, mechanical devices, and physical therapy used for prolapse treatment. [DOI: 10.1115/1.4045707]

Introduction

Pelvic organ prolapse (POP) is a disorder that affects up to 50% of women [1]. Patients diagnosed with POP typically experience symptoms such as incontinence, lower back pain, physical discomfort, and poor self-image [2,3]. Risk factors such as aging, high body mass index, and high infant birth weight have been identified [4], but the etiology of POP still remains unknown, making the development and implementation of effective treatments difficult. It has been estimated that more than $1 billion is spent annually on surgical treatments for POP [5] and approximately 30% of surgical patients require additional surgeries in their lifetime [6]. Alternatives to surgical treatments, such as physical therapy, have been explored, but demonstrated limited success [7].

Research to determine the possible causes of POP and improve current treatment is especially needed given the warnings issued by the United States Food and Drug Administration (FDA), which has publicized the risks associated with synthetic surgical meshes [8]. Very recently (April 2019), the FDA has also banned the marketing of several meshes for implantation in the vaginal wall. To engineer biologically compatible implant materials and develop alternative treatments for POP, the mechanical behavior of the vaginal tissue needs to be thoroughly investigated. Several studies have focused on characterizing the elastic properties of the vagina via uniaxial tests using either cadaveric human tissue [9–15] or tissue from

animal models [16–21]. In addition, the influence of pregnancy, parity, menopause, aging, and prolapse on the elasticity of the vaginal tissue has previously been investigated and reviewed [22].

The viscoelastic properties of vaginal tissue have been also studied but to a much lesser extent. Peña et al. [9] have investigated the strain-rate dependent and stress relaxation properties of prolapsed human vaginal tissue via uniaxial tests, developing a constitutive model that describes the collected experimental data. The softening behavior of the prolapsed human vaginal tissue under uniaxial cyclic loading was found to be anisotropic in a follow-up study by Peña et al. [13]. Although uniaxial tests have provided valuable data, biaxial tests are physiologically more relevant since the vaginal is primarily loaded in vivo in two directions: the longitudinal direction (LD) and the circumferential direction (CD). For this reason, the biaxial elastic properties of vaginal tissue have been recently evaluated in a small number of studies [18,20,21] but, to our knowledge, there are no studies investigating the biaxial viscoelastic properties of the vagina.

In this study, we determine, for the first time, the biaxial stress relaxation properties of vaginal tissue isolated from healthy pubertal gilts. Gilts, young female pigs that have not farrowed, are selected as animal models due to established histological similarities between porcine and human vaginas [21,23]. This selection is further justified by our need for controlling the health, age, and reproductive history of the animals. Vaginal tissue from gilts was subjected to planar equi-biaxial tensile testing to characterize potential differences in the stress relaxation properties in the LD

and CD while the applied strain in the two directions is measured using the digital image correlation (DIC) method. The findings of this study will provide insight into improving current conservative therapies, surgical methods, and mesh materials for prolapse by providing new viscoelastic experimental data for the vaginal tissue.

Methods

Specimen Preparation. This study was conducted with the approval of the Institutional Animal Care and Use Committee (IACUC) at Virginia Tech. Entire vaginal tracts were isolated from five pubertal (approximately six month old) gilts, immediately post euthanasia. Each vaginal tract was then cut longitudinally along the urethra and flattened out. Twenty square specimens, with approximately 30 mm × 30 mm surface area and sides oriented along the LD and CD of the vagina, were obtained from random anatomical locations within the organs (Figs. 1(a)–1(c)). Three specimens were isolated from four gilts, and eight specimens were isolated from one gilt. Specimens were hydrated with 1× phosphate buffer solution (PBS), wrapped in 1× PBS-soaked gauze, and stored at −20 °C until mechanical testing. On the day of testing, each specimen was thawed at room temperature and hydrated in 1× PBS with 1% methylene blue dye (Fisher Science Education, Nazareth, PA). Thickness was measured in four locations along each specimen using a low-force digital caliper under 50 g compressive load (Absolute Low Force Caliper Series 573, Mitutoyo, Kawasaki, Japan). The average thickness (±standard deviation) was found to be 2.27 ± 0.42 mm. Two pairs of safety pins, each pair connected by 4.0 cm long
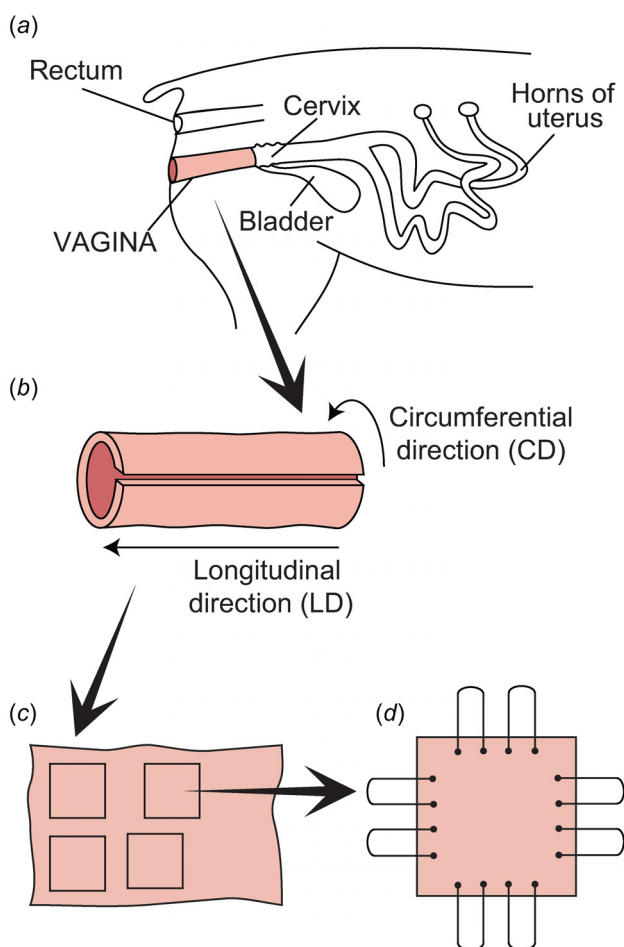

Fig. 1 (a) Position of the vagina in relation to other notable organs of the pelvic floor in the swine; (b) LD and CD of the vagina; (c) multiple square specimens isolated from one vaginal tract with sides oriented in the LD and CD; and (d) clamping method consisting of four pins inserted along each side of the specimen
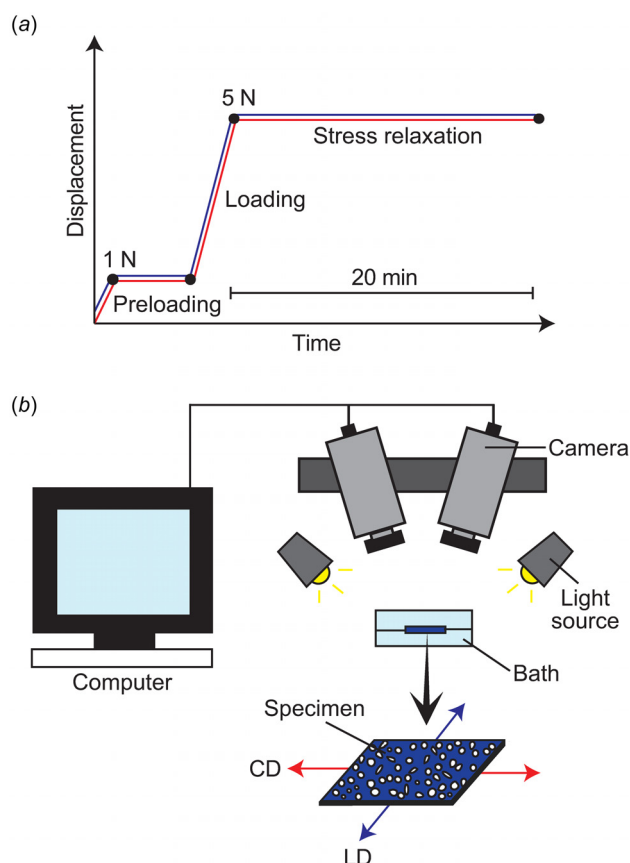

Fig. 2 (a) Experimental protocol for one test. The specimen was preloaded to 1 N in the LD and CD and held at that displacement for 300 s. It was then stretched at a rate of 0.1 mm/s until a load of 5 N was reached in both the LD and CD. The displacements reached by the specimen in the LD and CD at 5 N loads were held constant for 20 min. (b) Schematics of the strain measurement system showing the speckled specimen.

fishing line, were fastened along each edge of the specimen (Fig. 1(*d*)). The specimen was speckled with white spray paint (Rustoleum, Vernon Hills, IL) to create a random dot pattern suitable for DIC strain measurements [24].

Mechanical Testing. The speckle-painted specimens were mounted to a planar biaxial tensile testing system (Instron, Norwood, MA) with custom-made grips, and kept hydrated in a bath of 1× PBS for the entire duration of the tests. The system was equipped with 50 N load cells (accuracy ±0.05 N, Instron, UK). Each test consisted of three phases: preloading phase, loading phase, and stress relaxation phase (Fig. 2(*a*)). During preload, specimens were loaded up to 1 N in both the LD and CD and allowed to rest for 5 min. During loading, the specimens were stretched equi-biaxially at a rate of 0.1 mm/s until a 5 N load was recorded in both directions. During stress relaxation, the displacements that were achieved at 5 N load in the LD and CD were held constant for 20 min.

Force data were recorded during the loading and stress relaxation phases of the tests. Nominal axial stress data in the LD or CD were computed by dividing the axial force data by the undeformed cross-sectional area that was perpendicular to the LD or CD, respectively. For each specimen, the undeformed cross-sectional area was calculated as the product of average thickness and distance between pins. The distance between pins was measured using ImageJ (National Institutes of Health, Madison, WI). The cross-sectional area was found to be 67.58 ± 18.85 mm^2 along the LD and 64.75 ± 17.58 mm^2 along the CD. Hereafter, the nominal axial stress in one axial direction will be referred simply as stress in that direction.

Non-contact strain measurements were performed throughout the loading and stress relaxation phases of the tests using a 3D DIC system (Vic-3D, version 8, Correlated Solutions, Columbia, SC) (Fig. 2(*b*)). The DIC system consisted of two CMOS cameras (Basler ace acA2440-75μm, Basler, Inc., Exton, PA) fit with *c*-mount lenses (Xenoplan 2.8/50 Schneider Optics, Inc., Hauppauge, NY). Specifically, high-resolution (2448×2048 pixels) images were captured at a rate of five frames per second for each specimen. Local axial Lagrangian strains in the LD and CD
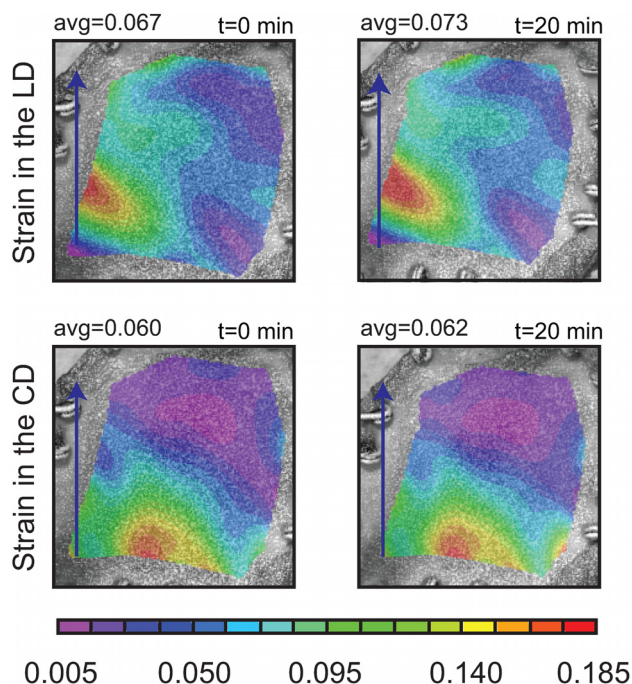
were then calculated over a square region in the center of each specimen using the 3D DIC system software (Vic-3D, version 8, Correlated Solutions, Columbia, SC) and averaged to compute a single average axial Lagrangian strain value along the LD and a single average Lagrangian strain value along the CD at each time point during testing. The average axial Lagrangian strain calculated for one specimen in each of the axial directions will be further referred simply as strain in that direction.

Data Analysis. Statistical analysis was performed using MINITAB statistical software (Minitab, Inc., version 19.1.1, State College, PA) with the significance level, α, set to 0.01. To determine if the strain during stress relaxation remained constant over time and was different in the LD and CD, a two-way analysis of variance (ANOVA) with repeated-measures was used. Specifically, the strains in the LD and CD were compared at the beginning ($t = 0$ min) and the end ($t = 20$ min) of stress relaxation. Similarly, a two-way ANOVA with repeated-measures was used to compare the stresses in the LD and CD at the beginning and the end of stress relaxation.

In order to compare the stress relaxation properties in the LD and CD for each specimen, the nonlinear stress versus time curves generated from the collected data in each direction were normalized and linearized using the method presented by Peleg [25]. Briefly, for each direction, the $(\sigma(t), t)$ data points were transformed into the $((\sigma_o t/(\sigma_o - \sigma(t))), t)$ data points, where t is the time, $\sigma_o = \sigma(0)$ is the stress at the beginning ($t = 0$) of the stress relaxation test, and $\sigma(t)$ is the stress at any time $t > 0$ during the stress relaxation test. For each specimen, the two sets of $((\sigma_o t/(\sigma_o - \sigma(t))), t)$ data points, one in the LD and one in the
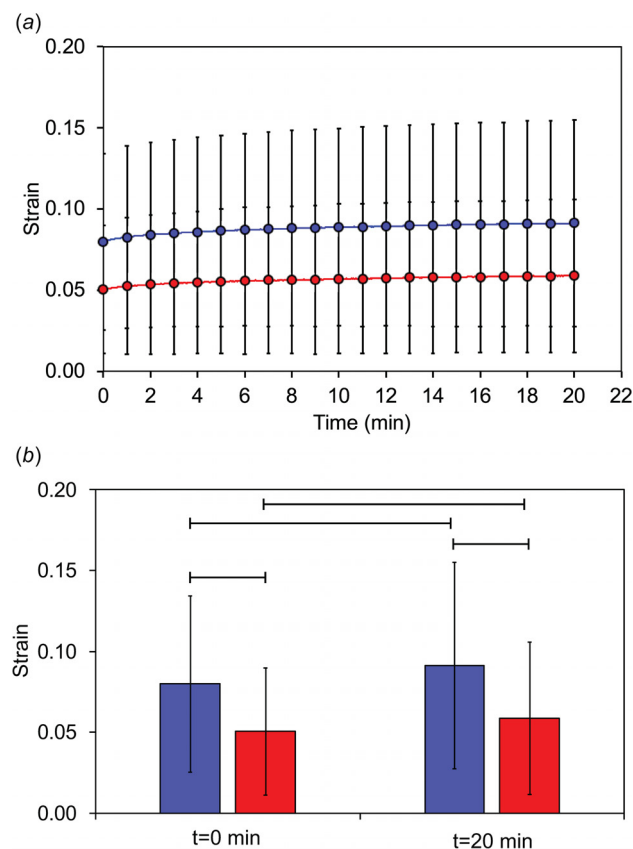

Fig. 3 Strain maps in the LD and CD for a representative specimen at the beginning ($t = 0$ s) and at the end ($t = 20$ min) of a representative stress relaxation test. The blue arrows indicate the LD.

Fig. 4 (*a*) Average strain (±S.D.) over time in the LD (blue squares) and CD (red circles) during stress relaxation tests ($n = 20$ specimens) and (*b*) comparison of strain in the LD (blue) and CD (red) at the beginning ($t = 0$ min) and end ($t = 20$ min) of stress relaxation. For all comparisons, $p > 0.01$. For interpretation of the references to color in this figure caption, the reader is referred to the web version of this article.

CD, were compared using linear regression analysis. Specifically, the intercepts k_1 and the slopes k_2 of the lines with equation $k_1 + k_2 t$ in the $((\sigma_o t/(\sigma_o - \sigma(t))), t)$ plane in the LD and CD were compared. The reciprocal of k_1 is the initial decay rate and the reciprocal of k_2 is the asymptotic value of the normalized relaxation parameter $((\sigma_o - \sigma(t))/\sigma_o)$. The constant k_2 represents the degree of solidity and it varies between $k_2 = 1$ for a material that is truly liquid (i.e., the stress reaches 0 during stress relaxation) to $k_2 \rightarrow \infty$ for an ideal elastic solid (i.e., the stress does not decrease at all during stress relaxation) [25]. All data were presented as mean-± standard deviation (S.D.).

Results

Figure 3 shows the strain map and average strains in the LD and CD for one specimen at the beginning ($t = 0$ min) and at the end ($t = 20$ min) of stress relaxation. A small increase in strains over time as well as a small difference in strains in the LD and CD was detected. Figure 4 presents the large variation in average strain (±S.D.) at several time points throughout stress relaxation in both the LD and CD. From the beginning ($t = 0$ min) to the end ($t = 20$ min) of the stress relaxation, the strain in the LD increased from 0.055 ± 0.022 to 0.091 ± 0.070, while strain the CD increased from 0.043 ± 0.030 to 0.058 ± 0.048. Despite the observed increase in strain with time and the higher strain in the LD, the strain values at $t = 0$ min and at $t = 20$ min in each direction and the strain values in the LD and CD were not found to be statistically different ($p > 0.01$ for both comparisons).

The stress relaxation data in the LD and CD from all tested specimens are presented in Fig. 5. The initial stress varied among specimens in both directions despite the fact that the initial loads were relatively constant (approximately 5 N) at the beginning of the stress relaxation tests. This difference is due to the variation in cross-sectional areas of the specimens. In Fig. 6(a), the average stress (±S.D.) at several time points during the stress relaxation tests, in both the LD and CD, are reported. Initial stress decreased from 71.59 ± 14.91 kPa to 36.09 ± 9.35 kPa in the LD, and from 75.63 ± 18.53 kPa to 40.59 ± 10.17 kPa in the CD. Average stresses were found to be different between the LD and CD at both the initial time point ($t = 0$ min) and final time point ($t = 20$ min) as well as between these time points along each direction ($p \ll 0.001$) (Fig. 6(b)).

The normalized and linearized stress versus time data in the LD and CD for one representative specimen are reported in Fig. 7. The regression lines that were used to compare the two sets of data for this representative specimen are also presented ($R^2 = 0.995$, $p \ll 0.001$). The intercept k_1 and the slope k_1 of the two lines were found to be significantly different. Specifically, the slope k_2 was higher in the CD indicating "more solidity" and less stress relaxation in such direction. For each specimen, the regression lines were found to be statistically different ($p \ll 0.001$). The slopes and intercepts of the regression lines describing the stress relaxation behavior were different in the LD and CD. However, while the slopes and intercepts were higher in the CD for most specimens, the intercepts were higher in the LD for seven specimens and, for four of these seven specimens, the slopes were also higher. In Fig. 8, the transformed stress versus time data for all the specimens in the LD and CD are shown. The lines having the average intercepts and slopes in the LD and CD are also presented. The slope k_2 appears to be higher in the CD. The average k_1 and k_2 values in the LD and CD as well as the average R^2 value
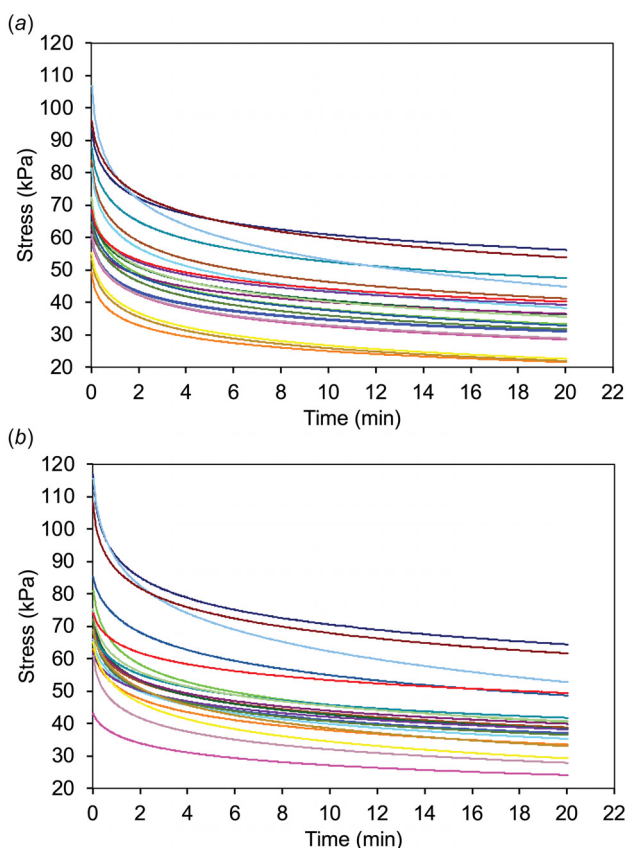

Fig. 5 Stress versus time data collected from $n = 20$ specimens during stress relaxation tests in the (a) LD and (b) CD. Data in the LD and CD collected from the same specimens are reported using the same colors. For interpretation of the references to color in this figure caption, the reader is referred to the web version of this article.
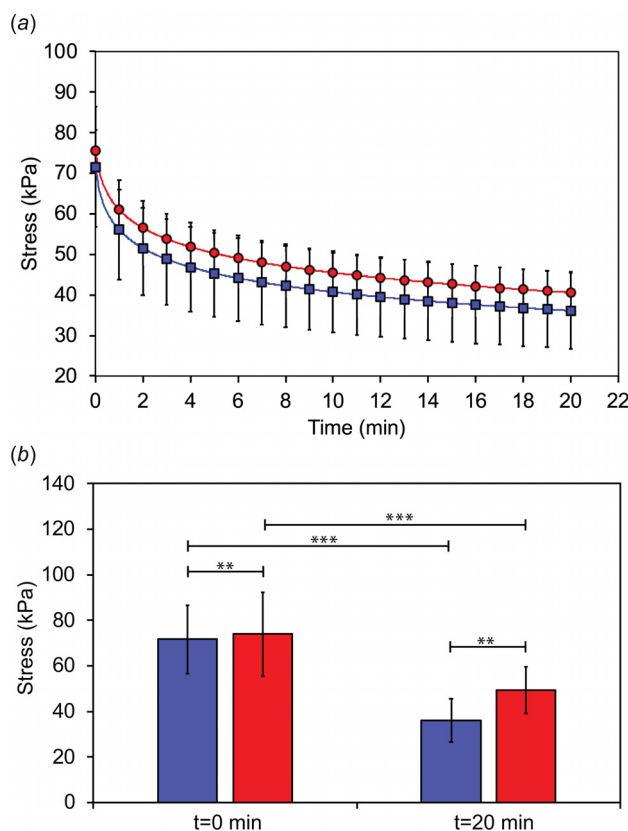

Fig. 6 (a) Average stress (±S.D.) over time in the LD (blue squares) and CD (red circles). (b) Comparison of stresses in the LD (blue) and CD (red) at the beginning ($t = 0$ min) and end ($t = 20$ min) of stress relaxation (**, $p < 0.01$, ***, $p < 0.001$). For interpretation of the references to color in this figure caption, the reader is referred to the web version of this article.
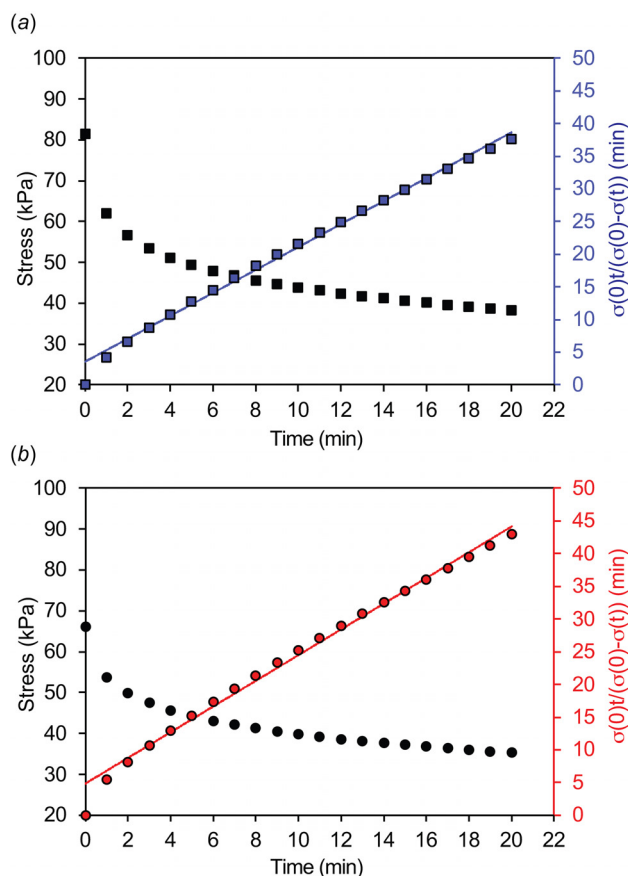
(a)

(b)

Fig. 7 Stress versus time data and linearized data using Peleg's approach with regression lines for one representative specimen. (a) Data in the LD with initial strain of 0.149, $k_1 = 3.80$ min, and $k_2 = 1.83$ and (b) data in the CD with initial strain of 0.065, $k_1 = 6.45$ min, and $k_2 = 2.08$ ($R^2 = 0.995$, $p \ll 0.001$).

computed from the linear regression analyses of $n = 20$ specimens are reported in Table 1.

Discussion

Our stress relaxation tests started when both the axial loads along the LD and CD reached 5 N. The 5 N load level was selected based on preliminary studies conducted in our lab showing that, at this load level, the swine vaginal tissue was subjected
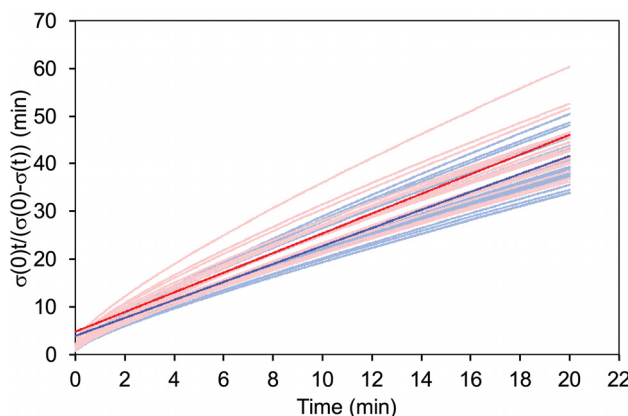

Fig. 8 Linearized stress versus time data using Peleg's approach in the LD (light blue curves) and CD (light red curves) with regression lines in the LD (dark blue line) and CD (dark red line). Average k_1 and k_2 values are reported in Table 1. For interpretation of the references to color in this figure caption, the reader is referred to the web version of this article.

Table 1 Mean ($\pm$S.D.) of the parameters k_1 and k_2 that resulted from the linear regression analysis of the transformed stress relaxation data in the LD and CD.

Mean $\pm$ S.D.	LD	CD
k_1 (min)	3.91 ± 0.67	4.79 ± 1.26
k_2	1.89 ± 0.22	2.06 ± 0.32

The average R^2 computed over $n = 20$ specimens was 0.996 and $p \ll 0.001$ for the comparison of the two regression lines.

to comparable strains in the LD and CD [21]. In this study, achieving comparable strains in both loading directions was important to determine potential differences in the resulting stress relaxation behavior between the LD and CD. By using the DIC methods during stress relaxation (Fig. 3), we confirmed that the difference between strains in the LD and CD was not statistically significant and the strain along each loading axis remained effectively constant during the stress relaxation test, as one would expect (Fig. 4). However, it is worth noting that there was large variation in the strains achieved by the different specimens, which was most likely due to inter specimen variability.

The average stress decreased by $49.91 \pm 5.81\%$ and $46.22 \pm 5.54\%$ in the LD and CD, respectively, at the end of the stress relaxation test, after 20 min (Fig. 6). This decrease in stress is comparable to the decrease in stress reported by Peña et al. for human vaginal tissue [9]. In the study by Peña et al., the stress in the LD decreased by 50–60% after 15 min at strains that were much higher than those used in our study. The small difference in the results may be attributed not only to the difference in experimental methods (uniaxial versus biaxial tests, open air versus PBS test environment) and tissues (prolapsed versus healthy, humans versus gilts) but also to the applied strain. Indeed, the average strain applied to our specimens in the LD was 8%, which is much lower than the 30–40% strains used by Peña et al. [9].

We normalized and linearized the stress relaxation data as done by Peleg [25] in order to statistically compare the stress relaxation behavior in the LD and CD (Figs. 7 and 8). The stress relaxation was found to be statistically different in the two directions with the model parameters k_1 and k_2 being higher in the CD for most specimens. The reciprocal of k_1 defines the initial stress decay rate so that lower value of k_1 in the LD indicated that the initial stress decay rate was higher in the LD. Moreover, since the value of k_2 defines the resistance to stress relaxation and the reciprocal of k_2 represents the asymptotic value of the normalized relaxation parameter $((\sigma_o - \sigma(t))/\sigma_o)$, higher value of k_2 in the CD meant that the specimen behaved more like a solid than a liquid in the CD, reaching a lower stress value after 20 min. The reason for the difference in stress relaxation in the two directions is unknown but it is likely due to the microstructural organization of the vagina. Based on previous biaxial stress relaxation studies on the bladder [26,27], we speculate that the presence of more collagen fibers carrying load in the LD may cause a larger decrease in load in such direction.

While many studies on soft tissue stress relaxation have utilized the Prony series, which is analogous to a set of Maxwell elements in parallel, to capture the stress relaxation behavior [28], we preferred to use Peleg's model. The advantage of Peleg's model is that it requires only two parameters to describe the stress relaxation data in each direction. Most importantly, the comparison between the stress relaxation behaviors in the two directions can be carried out by statistically comparing two regression lines. We did attempt to use the one-term Prony series to analyze the data, but the one-term Prony series with two parameters did not fit the data as well as Peleg's model. Notably, a two-term Prony series modeled the experimental data sufficiently well, but it required four instead of two parameters with little improvement over the Peleg's model. In general, as the number of parameters increases in a model, the estimation of the parameters from the data become

more ambiguous and the uniqueness of such parameters may not be guaranteed. Thus, for the purpose of comparing experimental data in two directions, we believe that the Peleg's model offers some clear advantages over the more common Prony series.

We have chosen to use the pubertal gilt as an animal model since the swine are similar to humans in vaginal tissue composition [21,23], cost-effective to raise, and provide large tissue specimen for mechanical testing. There is an added benefit to using swine for POP research: unlike other animal models (e.g., mice and rats), swine spontaneously develop POP [29]. Pubertal gilts, specifically, provide vaginal tissue that has not yet been altered by parity and older age, which are factors that increase the risk of POP in humans [30]. Therefore, we can assume that the stress relaxation properties we have determined represent properties of healthy vaginal tissue. Mechanically, the similarities between swine and human vaginal tissue have not yet been explored. Although the stress relaxation reported by Peña et al. [9] is similar to the one reported in this study, a thorough evaluation of the swine as a suitable model for studying POP in women should be performed. This can be accomplished by directly comparing the elastic and viscoelastic properties of both human and swine tissues using similar experimental methods and protocols.

The muscularis layer of the vagina is composed of two distinct sublayers of smooth muscle cells: an inner circumferential layer and an outer longitudinal layer. These sublayers determine the contractile properties of the entire vagina. Here, we have ignored the contribution of smooth muscle cell activation on the biaxial stress relaxation properties of the vagina since the organ was not tested in the active state. The viscoelastic properties of the vagina may be different in the active and passive states and the anisotropic behavior could even change with different activation methods [20]. Thus, future tests should focus on quantifying the biaxial stress relaxation properties of the vaginal wall in both the active and passive states. This is especially important since the content of smooth muscle cells significantly decreases in women with vaginal wall prolapse compared to women without prolapse [31,32], possibly leading to alterations of the active mechanical properties of the vaginal wall.

In order to reveal the potential nonlinear viscoelasticity of the vaginal tissue, experiments that probe the stress relaxation behavior at multiple strain levels must be carried out [33,34]. In our study, all the specimens were subjected to comparable biaxial strain levels since our main goal was to obtain the largest number of specimens for a meaningful comparison of stress relaxation properties in the LD and CD. For this reason, no conclusion could be drawn about the strain dependency of the stress relaxation properties of the vagina. Of course, additional experimental studies should be conducted to fully characterize the viscoelastic properties of the vagina in gilts and advance our limited understanding of the material properties of this organ. These future investigations can build upon the study that is presented here, moving toward the development of improved treatment strategies for vaginal prolapse.

Our reported variability in the stress relaxation behavior may be, in part, due to the random anatomical locations of the tested specimens within the vagina. Some studies have suggested mechanical differences of the anterior/posterior regions of the human vagina [11,35] and distal/proximal regions of the ovine vagina [36]. Others have indicated no differences in such properties based on the anterior/posterior location of the tested specimens for the ovine vagina [16]. The stress relaxation properties of the vaginal tissue may also vary from gilt to gilt. Notably, when grouping the collected data by gilt, we found that the intercepts k_1 and the slopes k_2 of the regression lines that capture the stress relaxation data in the LD and CD were significantly different ($p \ll 0.001$) for all the gilts but one. However, we had no clinical explanation that would allow us to exclude data from this gilt from our results. Experimental studies, which combine mechanical testing and microstructural analysis, should be conducted to reveal the possible sources of variability in the stress relaxation properties of the vaginal tissue.

Treatment options for POP include surgery, mechanical devices, and conservative therapies. The success of these different types of treatments requires knowledge of the mechanical properties of healthy vaginal tissue, so that prolapsed tissue can be somewhat restored to a healthy state. For example, current surgical methods utilize mesh and implant materials for prolapsed repair that may relax either isotropically or anisotropically [37]. Our study has found that, at least ex vivo in healthy pubertal gilts, stress relaxation of the vaginal tissue occurs anisotropically. If confirmed in vivo in human subjects, these findings indicate a need for viscoelastic mesh and implant materials that also relax anisotropically so as to be mechanically compatible with the host tissue.

Conclusions

Although POP affects up to 50% of women [1], little research has been done to measure the mechanical properties of the vaginal tissue, making the development and implementation of effective treatments difficult. This study presented the first ex vivo biaxial characterization of the stress relaxation properties of the healthy vagina using gilts as animal models. Full-field strain measurements confirmed that the applied strains in the LD and CD were not statistically different and remained almost constant during stress relaxation. Our findings indicated that the stress relaxation behavior of the vaginal tissue was significantly different in the LD and CD. Overall, the vaginal tissue relaxed more in the LD, exhibiting higher initial stress decay and lower asymptotic stress in such direction. These results could have implications in the design of new therapies, surgical methods, and mesh implants for POP treatment.

References

[1] Barber, M. D., and Maher, C., 2013, "Epidemiology and Outcome Assessment of Pelvic Organ Prolapse," Int. Urogynecology J., 24(11), pp. 1783–1790.
[2] Jelovsek, J. E., and Barber, M. D., 2006, "Women Seeking Treatment for Advanced Pelvic Organ Prolapse Have Decreased Body Image and Quality of Life," Am. J. Obstet. Gynecol., 194(5), pp. 1455–1461.
[3] Barber, M. D., 2005, "Symptoms and Outcome Measures of Pelvic Organ Prolapse," Clin. Obstet. Gynecol., 48(3), pp. 648–661.
[4] Swift, S., Woodman, P., O'Boyle, A., Kahn, M., Valley, M., Bland, D., Wang, W., and Schaffer, J., 2005, "Pelvic Organ Support Study (POSST): The Distribution, Clinical Definition, and Epidemiologic Condition of Pelvic Organ Support Defects," Am. J. Obstet. Gynecol., 192(3), pp. 795–806.
[5] Subak, L. L., Waetjen, L. E., Van Den Eeden, S., Thom, D. H., Vittinghoff, E., and Brown, J. S., 2001, "Cost of Pelvic Organ Prolapse Surgery in the United States," Obstet. Gynecol., 98(4), pp. 646–651.
[6] Olsen, A. L., Smith, V. J., Bergstrom, J. O., Colling, J. C., and Clark, A. L., 1997, "Epidemiology of Surgically Managed Pelvic Organ Prolapsed and Urinary Incontinence," Obstet. Gynecol., 89(97), pp. 501–506.
[7] Hagen, S., and Stark, D., 2011, "Conservative Prevention and Management of Pelvic Organ Prolapse in Women," Cochrane Database Syst. Rev., (12), pp. 1–69.
[8] FDA, 2011, "Urogynecologic Surgical Mesh: Update on the Safety and Effectiveness of Transvaginal Placement for Pelvic Organ Prolapse," Food and Drug Administration, Report.
[9] Peña, E., Calvo, B., Martínez, M. A., Martins, P., Mascarenhas, T., Jorge, R. M. N., Ferreira, A., and Doblaré, M., 2010, "Experimental Study and Constitutive Modeling of the Viscoelastic Mechanical Properties of the Human Prolapsed Vaginal Tissue," Biomech. Model. Mechanobiol., 9(1), pp. 35–44.

[10] Gilchrist, A. S., Gupta, A., Eberhart, R. C., and Zimmern, P. E., 2010, "Do Biomechanical Properties of Anterior Vaginal Wall Prolapse Tissue Predict Outcome of Surgical Repair?," J. Urol., **183**(3), pp. 1069–1073.

[11] Jean-Charles, C., Rubod, C., Brieu, M., Boukerrou, M., Fasel, J., and Cosson, M., 2010, "Biomechanical Properties of Prolapsed or Non-Prolapsed Vaginal Tissue: Impact on Genital Prolapse Surgery," Int. Urogynecology J., **21**(12), pp. 1535–1538.

[12] Martins, P., Peña, E., Calvo, B., Doblaré, M., Mascarenhas, T., Jorge, R. N., and Ferreira, A., 2010, "Prediction of Nonlinear Elastic Behaviour of Vaginal Tissue: Experimental Results and Model Formulation," Comput. Methods Biomech. Biomed. Eng., **13**(3), pp. 327–337.

[13] Peña, E., Martins, P., Mascarenhas, T., Natal Jorge, R. M., Ferreira, A., Doblaré, M., and Calvo, B., 2011, "Mechanical Characterization of the Softening Behavior of Human Vaginal Tissue," J. Mech. Behav. Biomed. Mater., **4**(3), pp. 275–283.

[14] Rubod, C., Brieu, M., Cosson, M., Rivaux, G., Clay, J. C., De Landsheere, L., and Gabriel, B., 2012, "Biomechanical Properties of Human Pelvic Organs," Urology, **79**(4), pp. 17–968.

[15] Chantereau, P., Brieu, M., Kammal, M., Farthmann, J., Gabriel, B., and Cosson, M., 2014, "Mechanical Properties of Pelvic Soft Tissue of Young Women and Impact of Aging," Int. Urogynecology J. Pelvic Floor Dysfun, **25**(11), pp. 1547–1553.

[16] Rubod, C., Boukerrou, M., Brieu, M., Dubois, P., and Cosson, M., 2007, "Biomechanical Properties of Vaginal Tissue—Part 1: New Experimental Protocol," J. Urol., **178**(1), pp. 320–325.

[17] Feola, A., Moalli, P., Alperin, M., Duerr, R., Gandley, R. E., and Abramowitch, S., 2011, "Impact of Pregnancy and Vaginal Delivery on the Passive and Active Mechanics of the Rat Vagina," Ann. Biomed. Eng., **39**(1), pp. 549–558.

[18] Robison, K. M., Conway, C. K., Desrosiers, L., Knoepp, L. R., and Miller, K. S., 2017, "Biaxial Mechanical Assessment of the Murine Vaginal Wall Using Extension–Inflation Testing," ASME J. Biomech. Eng., **139**(10), p. 104504.

[19] Rynkevic, R., Martins, P., Hympanova, L., Almeida, H., Fernandes, A. A., and Deprest, J., 2017, "Biomechanical and Morphological Properties of the Multiparous Ovine Vagina and Effect of Subsequent Pregnancy," J. Biomech., **57**, pp. 94–102.

[20] Huntington, A., Rizzuto, E., Abramowitch, S., Del Prete, Z., and Vita, R. D., 2019, "Anisotropy of The? Passive and Active Rat Vagina Under Biaxial Loading," Ann. Biomed. Eng., **47**(1), pp. 272–281.

[21] McGuire, J. A., Abramowitch, S. D., Maiti, S., and Vita, R. D., 2019, "Swine Vagina Under Planar Biaxial Loads: An Investigation of Large Deformations and Tears," ASME J. Biomech. Eng., **141**(4), p. 041003.

[22] Baah-Dwomoh, A., McGuire, J., Tan, T., and Vita, R. D., 2016, "Mechanical Properties of Female Reproductive Organs and Supporting Connective Tissues: A Review of the Current State of Knowledge," ASME Appl. Mech. Rev., **68**(6), p. 060801.

[23] Gruber, D. D., Warner, W. B., Lombardini, E. D., Zahn, C. M., and Buller, J. L., 2011, "Anatomical and Histological Examination of the Porcine Vagina and Supportive Structures: In Search of an Ideal Model for Pelvic Floor Disorder Evaluation and Management," Female Pelvic Med. Reconstr. Surg., **17**(3), pp. 110–114.

[24] Lionello, G., Sirieix, C., and Baleani, M., 2014, "An Effective Procedure to Create a Speckle Pattern on Biological Soft Tissue for Digital Image Correlation Measurements," J. Mech. Behav. Biomed. Mater., **39**, pp. 1–8.

[25] Peleg, M., 1979, "Characterization of the Stress Relaxation Curves of Solid Foods," J. Food Sci., **44**(1), pp. 277–281.

[26] Nagatomi, J., Gloeckner, D. C., Chancellor, M. B., Degroat, W. C., and Sacks, M. S., 2004, "Changes in the Biaxial Viscoelastic Response of the Urinary Bladder Following Spinal Cord Injury," Ann. Biomed. Eng., **32**(10), pp. 1409–1419.

[27] Nagatomi, J., Toosi, K. K., Chancellor, M. B., and Sacks, M. S., 2008, "Contribution of the Extracellular Matrix to the Viscoelastic Behavior of the Urinary Bladder Wall," Biomech. Model. Mechanobiol., **7**(5), pp. 395–404.

[28] Fung, Y.-C., 1993, *Biomechanics: Mechanical Properties of Living Tissues*, Springer, New York, NY.

[29] Stock, J. D., Supakorn, C., Hostetler, C., and Stalder, K. J., 2017, "Prolapse Incidence in Swine Breeding Herds is a Cause for Concern," Open J. Vet. Med., **7**(8), pp. 85–97.

[30] MacLennan, A. H., Taylor, A. W., Wilson, D. H., and Wilson, D., 2000, "The Prevalence of Pelvic Floor Disorders and Their Relationship to Gender, Age, Parity and Mode of Delivery," BJOG, **107**, pp. 1460–1470.

[31] Boreham, M. K., Wai, C. Y., Miller, R. T., Schaffer, J. I., and Word, R. A., 2002, "Morphometric Analysis of Smooth Muscle in the Anterior Vaginal Wall of Women With Pelvic Organ Prolapse," Am. J. Obstet. Gynecol., **187**(1), pp. 56–63.

[32] Takacs, P., Gualtieri, M., Nassiri, M., Candiotti, K., and Medina, C. A., 2008, "Vaginal Smooth Muscle Cell Apoptosis is Increased in Women With Pelvic Organ Prolapse," Int. Urogynecology J., **19**(11), pp. 1559–1564.

[33] Davis, F. M., and De Vita, R., 2012, "A Nonlinear Constitutive Model for Stress Relaxation in Ligaments and Tendons," Ann. Biomed. Eng., **40**(12), pp. 2541–2550.

[34] Becker, W. R., and De Vita, R., 2015, "Biaxial Mechanical Properties of Swine Uterosacral and Cardinal Ligaments," Biomech. Model. Mechanobiol., **14**(3), pp. 549–560.

[35] Martins, P., Lopes Silva-Filho, A., Rodrigues Maciel da Fonseca, A. M., Santos, A., Santos, L., Mascarenhas, T., Natal Jorge, R. M., and Ferreira, A. J., 2013, "Biomechanical Properties of Vaginal Tissue in Women With Pelvic Organ Prolapse," Gynecol. Obstet. Invest., **75**(2), pp. 85–92.

[36] Ulrich, D., Edwards, S. L., Letouzey, V., Su, K., White, J. F., Rosamilia, A., Gargett, C. E., and Werkmeister, J. A., 2014, "Regional Variation in Tissue Composition and Biomechanical Properties of Postmenopausal Ovine and Human Vagina," PLoS One, **9**(8), p. e104972.

[37] Liang, R., Knight, K., Abramowitch, S., and Moalli, P. A., 2016, "Exploring the Basic Science of Prolapse Meshes," Curr. Opin. Obstet. Gynecol., **28**(5), p. 413.